Biophysical Chemistry 134 (2008) 214–224

Contents lists available at ScienceDirect

Biophysical Chemistry

journal homepage: http://www.elsevier.com/locate/biophyschem

Different urea stoichiometries between the dissociation and denaturation of tobacco mosaic virus as probed by hydrostatic pressure

Jose L.R. Santos [a], Ricardo Aparicio [b], Inés Joekes [b], Jerson L. Silva [c], Jose A.C. Bispo [a], Carlos F.S. Bonafe [a,*]

[a] Laboratório de Termodinâmica de Proteínas, Departamento de Bioquímica, Instituto de Biologia, Universidade Estadual de Campinas (UNICAMP), CP 6109, Brazil
[b] Departamento de Físico-Química, Instituto de Química, Universidade Estadual de Campinas (UNICAMP), Campinas, SP, 13083-970, Brazil
[c] Instituto de Bioquímica Médica, Centro Nacional de Ressonância Magnética Nuclear de Macromoléculas Jiri Jonas, Universidade Federal do Rio de Janeiro (UFRJ), Rio de Janeiro, RJ, 21941-590, Brazil

ARTICLE INFO

Article history:
Received 6 November 2007
Received in revised form 14 February 2008
Accepted 17 February 2008
Available online 25 February 2008

Keywords:
Tobacco mosaic virus
Virus denaturation
Urea-induced denaturation
High pressure-induced dissociation
High pressure-induced denaturation

ABSTRACT

Viruses are very efficient self-assembly structures, but little is understood about the thermodynamics governing their directed assembly. At higher levels of pressure or when pressure is combined with urea, denaturation occurs. For a better understanding of such processes, we investigated the apparent thermodynamic parameters of dissociation and denaturation by assuming a steady-state condition. These processes can be measured considering the decrease of light scattering of a viral solution due to the dissociation process, and the red shift of the fluorescence emission spectra, that occurs with the denaturation process. We determined the apparent urea stoichiometry considering the equilibrium reaction of TMV dissociation and subunit denaturation, which furnished, respectively, 1.53 and 11.1 mol of urea/mol of TMV subunit. The denaturation and dissociation conditions were arrived in a near reversible pathway, allowing the determination of thermodynamic parameters. Gel filtration HPLC, electron microscopy and circular dichroism confirmed the dissociation and denaturation processes. Based on spectroscopic results from earlier papers, the calculation of the apparent urea stoichiometry of dissociation and denaturation of several other viruses resulted in similar values, suggesting a similar virus–urea interaction among these systems.

1. Introduction

The thermodynamics of protein–protein interaction is of fundamental importance in the understanding of biological systems. Progress in this area has been accomplished through the use of high hydrostatic pressure, a tool that promotes dissociation of proteins without significant effects on their tertiary structure [1]. Pressure effects follow Lê Chatelier's principle, so the system tends to occupy lower volume. A key advantage of the hydrostatic pressure is that it does not significantly change the chemical composition of the solvents, or the internal energy of the protein [2–4].

In recent years, the use of high hydrostatic pressure combined with chemical agents has been used to study the thermodynamic stability of proteins [5]. This knowledge represents a special concern due to the fundamental biological functions of these structures. The combination of high pressure with urea was investigated with several viral particles [6–16], demonstrating that, in most cases, dissociation precedes denaturation with the increase of urea concentration. The decrease of infectivity is another important effect since this tool can be used for vaccine development [10,17,18].

In the present study we investigate the pressure and urea effects in tobacco mosaic virus (TMV). This classic cylindrical-shaped virus (40,000 kDa) consists of 2130 identical capsidic proteins of 17.5 kDa and a 6.4 kb RNA [19]. Previous studies of urea effects on TMV were performed by Stanley and Lauffer [20], who observed a decrease of viral infectivity after incubation in 6.0 mol/L urea. Blowers and Wilson [21] demonstrated that TMV "degradation" by urea occurs predominantly at the 5′ to 3′ end of its RNA. The combined effects of high pressure and urea, depending on urea concentration and pressure level, induced TMV dissociation and denaturation [9]. In this report, in the specific condition of 2.5 mol/L urea, the increase of pressure from 10^{-2} to 250 MPa induced a red shift of 1900 cm^{-1}, corresponding to a calculated degree of denaturation from 0 to 1.

Recently we determined the proton stoichiometry in the dissociation of an extracellular giant hemoglobin [22], and TMV [23] by high pressure at different pH values. Through this methodology we

* Corresponding author.
E-mail address: bonafe@unicamp.br (C.F.S. Bonafe).

0301-4622/$ – see front matter © 2008 Elsevier B.V. All rights reserved.
doi:10.1016/j.bpc.2008.02.010

extended our study determining the urea stoichiometry in dissociation and denaturation processes induced by high hydrostatic pressure. These processes were monitored by light scattering and center of mass of fluorescence and the products were analyzed by HPLC. Changes in the secondary structure were monitored by circular dichroism. Our findings aim to contribute to the understanding of the forces that maintain the stability of the native structure of TMV and the mechanism involved in the dissociation and denaturation processes.

2. Materials and methods

2.1. Chemicals

All reagents were of analytical grade. Distilled water was filtered and deionized through a Millipore water purification system (18 MΩ resistance). Unless stated otherwise, the experiments were done at 5 °C with 100 mmol/L Tris–HCl buffer, pH 7.0. Ultra pure urea was obtained from Sigma. The virus was isolated from Turkish tobacco plants infected with the common strain of the virus. The virus was purified as described by Asselin and Zaitlin [24].

2.2. Light scattering and fluorescence under pressure

The high-pressure system has been described elsewhere [25]. An ISS model HP high-pressure cell with sapphire windows connected to a pressure generator (HIP) was used. Light scattering and fluorescence were recorded with an Edinburgh FL 900 spectrofluorometer, equipped with a xenon lamp-source. The pressure system was automated and detailed by Santos et al. [23]. Light scattering at 340 nm was measured at an angle of 90 relative to the incident light using the same wavelength for the excitation and emission monochromators. We estimated the average molar mass based on intensity of light scattering (Eqs. (17)–(32) from [26]) at pressure p, S_p, calculating the respective degree of dissociation (α_p) as

$$\alpha_p = (S_i - S_p)/(S_i - S_f) \tag{1}$$

where S_f and S_i are the intensities of light scattering for the dissociated and associated forms, respectively [27].

The fluorescence data were studied by excitation of the virus at 280 nm, and emission was observed at 300–400 nm. Changes in the fluorescence spectra due to exposure of tryptophan residues were quantified by the spectral center of mass (ν_p).

$$\nu_p = \frac{\sum \nu_i F_i}{F_i} \tag{2}$$

where F_i, stands for the fluorescence emitted at wavenumber ν_i, and the summation is carried out over the range of appreciable values of F. The degree of denaturation at pressure p, $\alpha_{\mathrm{den},p}$ is related to ν by the expression

$$\alpha_{\mathrm{den},p} = \left[\frac{1 + Q(\langle \nu_p \rangle - \langle \nu_{\mathrm{des}} \rangle)}{(\langle \nu_n \rangle - \langle \nu_p \rangle)}\right]^{-1} \tag{3}$$

where Q is the ratio of the quantum yields of denatured and native forms, ν_p is the center of mass at pressure p, and ν_{des} and ν_n are the corresponding quantities for denatured and native forms.

2.3. Circular dichroism

TMV solutions (0.125 mg/mL) in 20 mmol/L sodium phosphate buffer, pH 7.0, at different urea concentrations were transferred to a 2 mm path-length quartz cuvette. Circular dichroism spectra in the wavelength range of 190 to 300 nm were acquired with a Jasco J-810 spectropolarimeter, model 1505 (Jasco Corp., Japan) using a bandwidth of 1 nm and a response time of 1 s.

Data collection was performed at room temperature with a scanning speed of 100 nm/min. A total of nine scans were accumulated for each sample and all the spectra were corrected by subtraction of buffer blanks.

2.4. Gel filtration

Size exclusion HPLC was performed in a Shimadzu HPLC system. A prepacked SynChropack GPC 1000 column (250×4.6 mm i.d.) (SynChrom, Inc., Linden, IN), was used for gel filtration. Elution of the samples was monitored by absorption at 280 nm. The void volume (V_0) of the column was measured with TMV before the application of pressure and the total volume (V_t) with a solution of human albumin. Extracellular hemoglobin (3300 kDa) from *G. paulistus* [27] was used as a molar mass standard in the presence of 0.1 mol/L calcium chloride.

2.5. Electron microscopy

Transmission electron microscopy was done in a Leo-902 microscope. The samples were fixed with 0.5% glutaraldehyde solution and after negative staining was done with 1% uranyl acetate.

2.6. Tryptophan classification

Tryptophan classes were assigned by visual inspection of the tryptophan environment according to the classification defined by Vivian and Callis [28]. PDB entries mentioned in "Table 2" of the referenced article were used for structural comparisons, as representative structures of the five classes proposed by the authors. PDBSET [29] was used for coordinate manipulations.

2.7. Theory

In the presence of urea, TMV exhibits dissociation at lower urea concentration, denaturating at higher levels [9]. Analogous to the effect of pH on TMV dissociation [23], the process can be written as

$$P_{2130}N + \upsilon U \overset{K}{\leftrightarrow} 2130PU_\sigma + N \tag{4}$$

where U, P, N and $P_{2130}N$ correspond, respectively, to urea, capsid protein, viral RNA and TMV whole particles, υ corresponds to the stoichiometric coefficient, and $\upsilon = 2130\sigma$. Here, the equilibrium constant of dissociation at atmospheric pressure is K, which corresponds to the ratio of rate constants of product and reagent formation, k_{+1}/k_{-1}. Even if the number of subunits that dissociates in the experimental conditions were different from that adopted here, the use of values lower than 2130 would yield very similar results for the apparent free energy, volume change of dissociation and urea mol per mol of subunits. For instance, if the number of subunits was 100 instead 2130, σ would change negligibly, as will be shown later. This behavior was mentioned in a previous report, for the proton stoichiometry of dissociation of a giant annelid hemoglobin [22]. According to HPLC data (Fig. 5), the stabilization of dissociated products suggests a steady-state condition [9,30], with an irreversible step due to a more profound change of conformation of free subunits, occurring the reaction $P \rightarrow^{k_2} P^*$, where k_2 corresponds to the rate constant of this process. The derived thermodynamic parameters are considered in the present work as apparent parameters, which are expressed with the superscript "*" (asterisk). The apparent constant of dissociation corresponds to $K^* = k_{+1}/(k_{-1} + k_2)$ [9]. We considered this condition also for process of denaturation that occurs from dissociated species P, the dissociated form, which is already combined with σ molecules of urea. Thus, the corresponding reaction becomes

$$PU_\sigma + \lambda U \overset{K_{\mathrm{den}}}{\leftrightarrow} PU_{\sigma+\lambda} \tag{5}$$

with equilibrium constant at atmospheric pressure, K_{den}. Here λ represents the stoichiometric coefficient of denaturation. The

proper apparent equilibrium constants of dissociation and denaturation are

$$K^* = \frac{[PU_\sigma]^{2130}[N]}{[P_{2130}N][U]^{\upsilon}} \tag{6}$$

and

$$K^*_{\mathrm{den}} = \frac{[PU_{\sigma+\lambda}]}{[PU_\sigma][U]^{\lambda}} \tag{7}$$

where we represent the denaturation process through the *den* index. For a given urea concentration, [*U*], it is possible to express the apparent dissociation constant $K^*_{[U]}$ as

$$K^*_{[U]} = K^*[U]^{\upsilon} = \frac{[P]^{2130}_{[U]}[N]_{[U]}}{[P_{2130}N]_{[U]}} \tag{8}$$

where the respective species in the defined ligand concentration is represented with the index "[*U*]". The apparent free energy of dissociation is

$$\Delta G^*_{[U]} = \Delta G^*_{U_1} - \upsilon RT\ln[U] \tag{9}$$

where *R* is the gas constant, *T* is the absolute temperature, and $\Delta G^*_{U_1}$ is the corresponding apparent energy change of dissociation at [*U*]=1 mol/L, since here we are considering molar bases.

The correlation between the apparent dissociation constant at a urea concentration of [*U*], at pressure *p* and atmospheric pressure, can be obtained from the respective apparent free energies of dissociation, $\Delta G^*_{[U],p}$ and $\Delta G^*_{[U]}$, as

$$\Delta G^*_{[U],p} = \Delta G^*_{[U]} + p\Delta V^* \tag{10}$$

where ΔV^* represent the apparent volume change of dissociation. This relation gives

$$K^*_{[U],p} = K^*_{[U]}\exp\left(-p\Delta V^*/RT\right) = \frac{[P]^{2130}_{[U],p}[N]_{[U],p}}{[P_{2130}N]_{[U],p}}. \tag{11}$$

This relation, written in terms of the corresponding degree of dissociation at pressure *p*, estimated based on light scattering data, Eq. (1), at the defined urea concentration, α_p, furnishes

$$K^*_{[U],p} = K^*_{[U]}\exp\left(-p\Delta V^*/RT\right) = \frac{2130^{2130}C^{2130}\alpha_p^{2131}}{1-\alpha_p} \tag{12}$$

where *C* is the total TMV concentration. Here we considered [*P*]= $2130\alpha_p C$, [*N*]=$\alpha_p C$ and $[P_{2130}N]=(1-\alpha_p)C$. The logarithmic form yields the linear relationship

$$\ln K^*_{[U],p} = \ln K^*_{[U]} - \frac{p\Delta V^*}{RT} = 2130\ln 2130 + 2130\ln C + 2131\ln\alpha_p - \ln(1-\alpha_p). \tag{13}$$

A plot of $\ln K^*_{[U],p}$ versus *p* results in a straight line, the linear and angular coefficients of which (Eq. (13)) furnish values for $\ln K^*_{[U]}$ that are used to calculate the values of $G^*_{[U]}$ and ΔV^*.

The denaturation of TMV, from Eq. (7), can be expressed for a defined urea concentration in a similar approach, so the respective apparent denaturation constant $K^*_{\mathrm{den},[U]}$ is

$$K^*_{\mathrm{den},[U]} = K^*_{\mathrm{den}}[U]^{\lambda} = \frac{[PU_{\sigma+\lambda}]_{[U]}}{[PU_\sigma]_{[U]}}. \tag{14}$$

The apparent free energy of denaturation becomes

$$\Delta G^*_{\mathrm{den},[U]} = \Delta G^*_{\mathrm{den},U_1} - \lambda RT\ln[U] \tag{15}$$

where $\Delta G^*_{\mathrm{den},U_1}$ is the apparent free energy of denaturation at [*U*]= 1 mol/L.

Analogous to the equations for dissociation, Eqs. (10)–(13), the apparent denaturation constant at a pressure *p* can be obtained

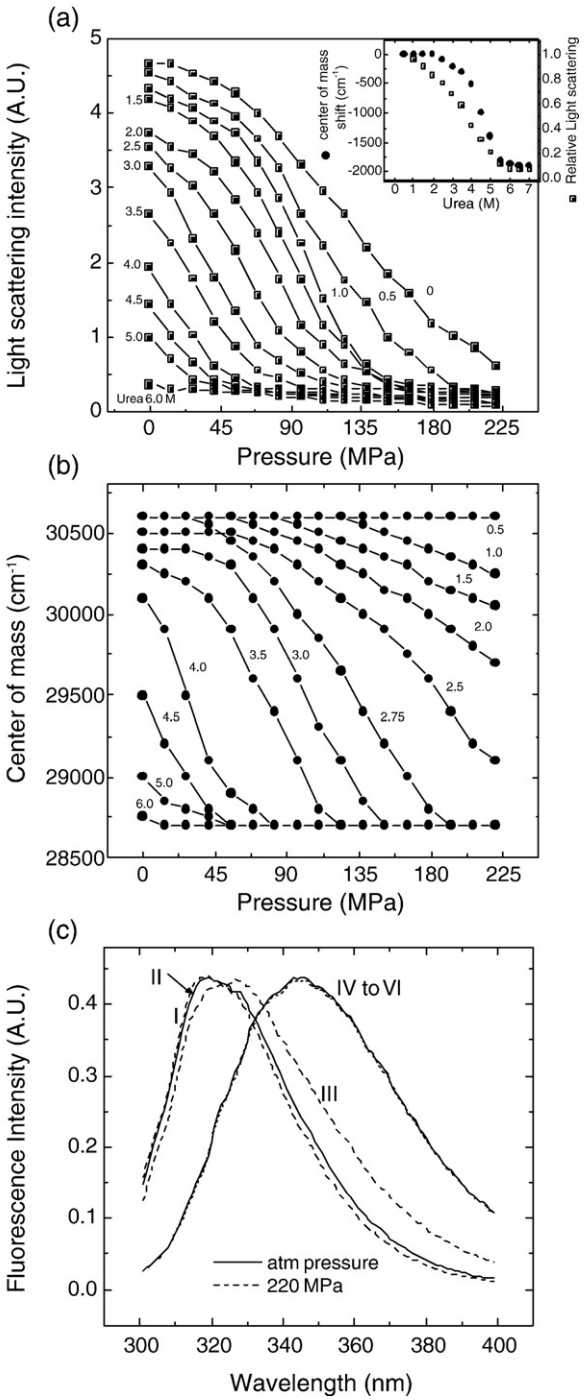

Fig. 1. Effect of pressure and urea on light scattering and fluorescence properties of TMV (0.25 mg/mL) in 100 mmol/L Tris–HCl buffer at pH 7.0 and at 5 °C. The data were obtained after 17 min incubation at each pressure value. The experiments were done in triplicate, and the standard deviations were smaller than the symbols. (a) Light scattering at 340 nm (A.U. = arbitrary units). Inset. Effect of urea on light scattering and center of mass of the fluorescence emission spectra (Eq. (3)) at atmospheric pressure. (b) Center of mass of emission fluorescence spectra (Eq. (2)), and (c) normalized emission fluorescence spectra of TMV in the absence of urea (I and II), and in the presence of 3.0 mol/L urea (III and IV) and 6.0 mol/L urea (V and VI). Excitation at 285 nm and emission at 300 to 400 nm.

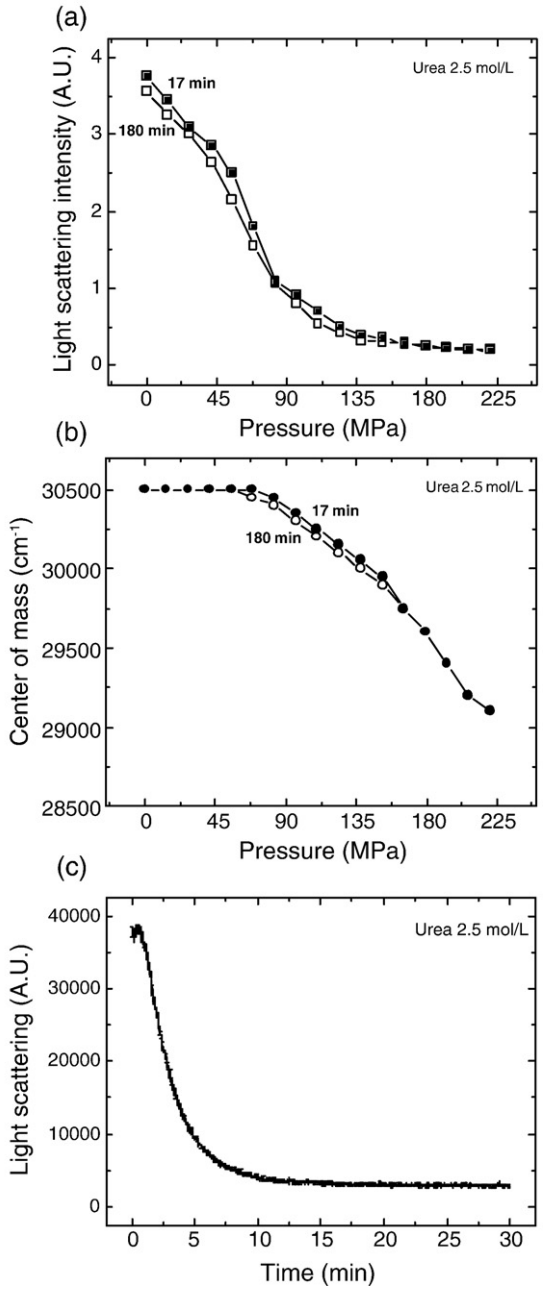

Fig. 2. Effect of pressure and 2.5 mol/L urea on (a) light scattering intensities and (b) center of mass of fluorescence emission spectrum according to Eq. (2) of TMV at two different time incubations, 17 and 180 min, and (c) effect of time on TMV at 2.5 mol/L urea pressurized from 0.1 to 220 MPa in 1.5 min. All other conditions are the same as Fig. 1.

through the respective apparent free energies of denaturation at a urea concentration of $[U]$ as

$$\Delta G^*_{\mathrm{den},[U],p} = \Delta G^*_{\mathrm{den},[U]} - P\Delta V^*_{\mathrm{den}} \tag{16}$$

where $\Delta V^*_{\mathrm{den}}$ represent the apparent volume change of denaturation. This relation gives

$$K^*_{\mathrm{den},[U],p} = K^*_{\mathrm{den},[U]} \exp\left(-p\Delta V^*_{\mathrm{den}}/RT\right) = \frac{[PU_{\sigma+\lambda}]_{[U],p}}{[PU_{\sigma}]_{[U],p}} \tag{17}$$

$$K^*_{\mathrm{den},[U],p} = K^*_{\mathrm{den},[U]} \exp\left(-p\Delta V^*_{\mathrm{den}}/RT\right) = \frac{\alpha_{\mathrm{den},p}}{1-\alpha_{\mathrm{den},p}} \tag{18}$$

$$\ln K^*_{\mathrm{den},[U],p} = \ln K^*_{\mathrm{den},[U]} - \frac{p\Delta V^*_{\mathrm{den}}}{RT} = \ln\alpha_{\mathrm{den},p} - \ln\left(1-\alpha_{\mathrm{den},p}\right). \tag{19}$$

It is important emphasize that the degree of denaturation, $\alpha_{\mathrm{den},p}$, Eq. (3), is based on fluorescence emission analysis. As in the case of the dissociation process, we obtain information related to the denaturation process by plotting $\ln K^*_{\mathrm{den},[U],p}$ *versus* p.

As mentioned above, considering a very different dissociation order, like $n=100$, apparent thermodynamic parameters such as ΔV^* or urea stoichiometry of dissociation per subunit, σ, will change negligibly. This can be verified if we consider that, generically, $\ln K^*_{[U],p}$, for dissociation order n, observing Eq. (13), will be

$$\ln K^*_{[U],p} = \ln K^*_{[U]} - \frac{p\Delta V}{RT} = n\ln n + n\ln C + (n+1)\ln\alpha_p - \ln\left(1-\alpha_p\right) \tag{20}$$

so, the $\Delta G^*_{[U]}$ at atmospheric pressure per subunit becomes

$$\Delta G^*_{[U]} = -RT\left(\ln n + \ln C + \frac{n+1}{n}\ln\alpha - \frac{1}{n}\ln(1-\alpha)\right). \tag{21}$$

Taking two different values of urea concentrations [U2] and [U1], the respective $\Delta\Delta G^*$ for dissociation, related to urea stoichiometry, from Eq. (9), $d\Delta G^*_{[U]}/d\ln[U] = -RT$, is

$$\Delta\Delta G^*_{[U]} = -RT\left(\frac{n+l}{n}\ln\frac{\alpha_{[U2]}}{\alpha_{[U1]}} - \frac{1}{n}\ln\frac{1-\alpha_{[U2]}}{1-\alpha_{[U]}}\right). \tag{22}$$

From these relations, taking two determined values of α as $\alpha_{[U2]}=0.3$ and $\alpha_{[U1]}=0.8$, substituting in Eq. (22) for $n=2130$, and calculating

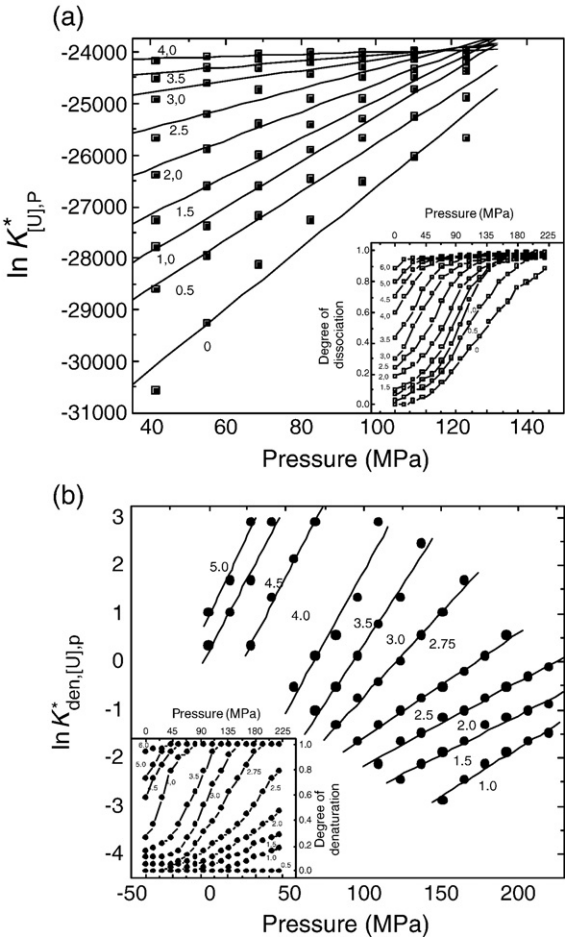

Fig. 3. Plot of $\ln K^*_{[U],p}$ (Eq. (13)), (a), and $\ln K^*_{\mathrm{den},[U],p}$ (Eq. (19)), (b), *versus* pressure, based on the respective degrees of dissociation and denaturation, inset (a) and (b). These latter plots were based on, respectively, the results of Fig. 1(a) (Eq. (1)), and Fig. 1(b). The data of Fig. 1b were based on Eq. (3), that considers the corrections according to the respective quantum yields, which in more extreme cases decreased by only about 15%.

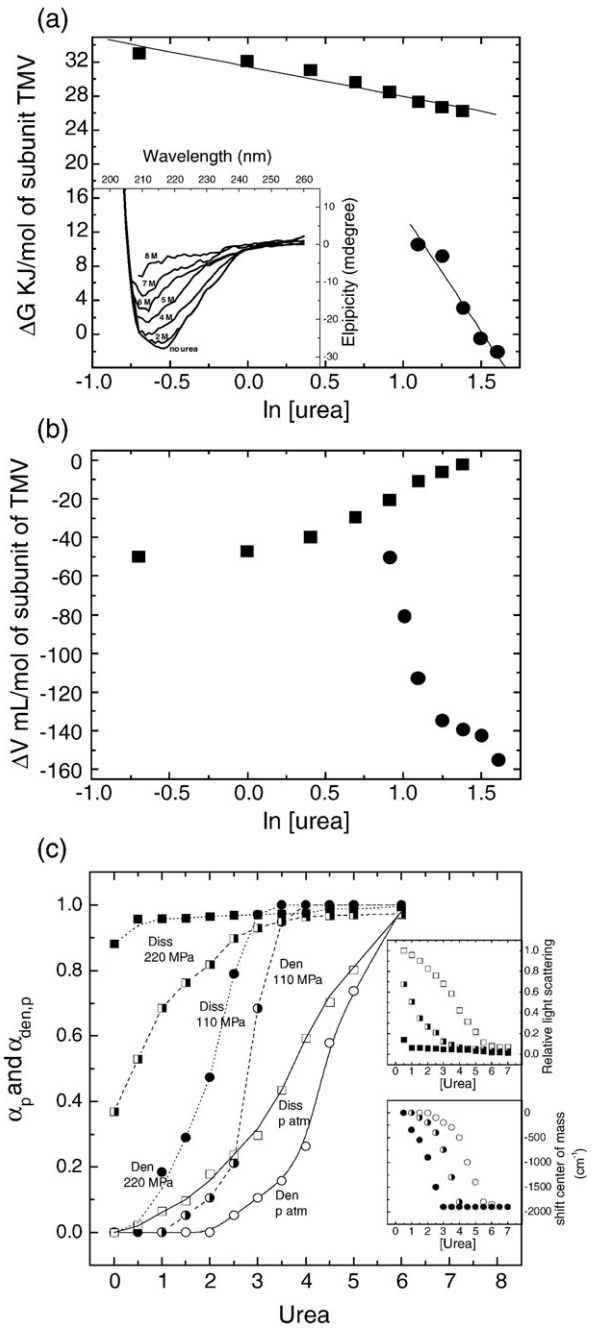

Fig. 4. Effect of urea (a) on the apparent Gibbs free energy of TMV dissociation (squares) and denaturation (circles), (b) on the apparent volume change of dissociation (squares) and denaturation (circles), and (c) on the degree of dissociation and denaturation of TMV at 0.1, 110 and 220 MPa (from Fig. 3 insets). The results for ΔG were obtained from the linear fitting shown in Fig. 3 (Eqs. (13) and (19)). (a) Inset: UV CD spectra of TMV at different urea concentrations. The spectra were obtained from 0.125 mg/mL TMV in 20 mmol/L sodium phosphate buffer, pH 7.0, using a 2 mm path-length quartz cuvette, at 5 °C. (c) Inset: effect of urea concentration on the light scattering and on the center of mass of the fluorescence emission spectra of TMV at 0.1, 110 and 220 MPa (from Fig. 1(a) and (b)).

for $n=100$, the value of $\Delta\Delta G^*_{[U]}$ increases only 1.17%, permitting the conclusion that the order of dissociation negligibly changes the urea stoichiometry per mol of subunits. The same can be verified for ΔV^* per mol of dissociated subunits.

3. Results

The effects of urea and pressure on light scattering and the center of mass of fluorescence spectra of TMV (pH 7.0) are shown in Fig. 1. The time interval chosen for incubation at each pressure value was 17 min because it corresponds to more than 98% of the attained point, according to experimental observations. This can be verified in Fig. 2, which shows that at 2.5 mol/L urea the pressure curves for 17 and 180 min were very similar based on light scattering, Fig. 2(a) and center of mass data, Fig. 2(b). Moreover the increase of pressure from atmospheric to 220 MPa, Fig. 2(c), results in highly significant dissociation, confirming that the experimental time at each pressure incubation of 17 min is very close to stabilization. Thus, dissociation and denaturation processes in the present report were performed in several intermediate points, each one very close to the equilibrium.

The light scattering intensity was reduced to buffer light scattering values with the increases of urea concentration and of pressure, Fig. 1(a), corresponding to significant dissociation. At concentrations of urea above 2.5 mol/L, a red shift of the center of mass up to 1900 cm^{-1} was observed, Fig. 1(a), indicating important aromatic residue exposure and suggesting denaturation. Some of respective normalized fluorescence emission spectra at different pressures and urea concentrations are shown in Fig. 1(c). Fig. 1(a) inset shows the isolated effect of urea at atmospheric pressure.

Fig. 3(a), inset and b, inset show the changes in the degrees of dissociation and denaturation (Eqs. (1) and (3)) of TMV based on the light scattering and center of mass data (Fig. 1). The corrections for denaturation data were according to the respective quantum yields, which in more extreme cases decreased only about 15%. From these data, the logarithmic forms of apparent dissociation and denaturation constants, $\ln K^*_{[U],p}$ and $\ln K^*_{den.[U],p}$ (Eqs. (13) and (19)), Fig. 3, were calculated. From the intercepts and slopes of these plots we obtained (Eqs. (10) and (16)) the free energies and the volume changes involved in these processes, Fig. 4(a) and (b). As can be observed, the apparent free energy of

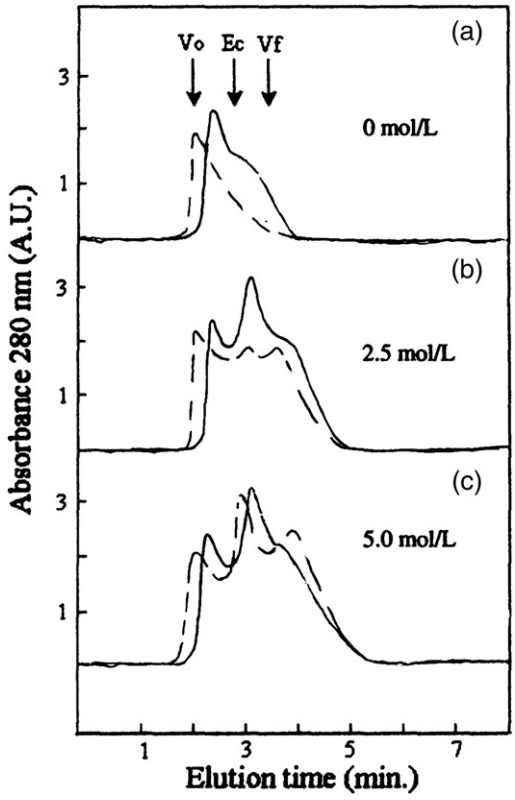

Fig. 5. Gel filtration HPLC analysis (GPC1000 column) of TMV subjected to high pressure at different urea concentrations. 100 mL of TMV (0.25 mg/mL, in 100 mmol/L Tris–HCl, pH 7.0) were injected and eluted at a rate flow of 0.3 mL/min. Dashed line: TMV at atmospheric pressure. Continuous line: TMV after 1.5 h at 220 MPa (a) in absence of urea, (b) at 2.5 mol/L urea and (c) at 5.0 mol/L urea. V_0 and V_t are the void and final volumes, respectively, and Ec is the elution point of extracellular hemoglobin (3300 kDa) from *G. paulistus* [27].

dissociation decreases from 35.16 to 26.18 kJ/mol of coat protein subunit, with the elevation of urea concentration from 0 to 4.0 mol/L. The apparent free energy of denaturation decreased from 10.5 to −2.15 kJ/mol of TMV with the elevation of urea concentration from 3.0 to 5.0 mol/L.

The apparent urea stoichiometries of dissociation and denaturation were obtained from Eqs. (9) and (15) using the slope of Fig. 4(a). The average number of urea mol bound during the dissociation and denaturation processes (ρ, and λ) were, respectively, 1.53 and 11.1 mol of urea/mol of TMV subunit. The calculated apparent volume changes of dissociation and denaturation, Eqs. (13) and (19), exhibit negative values, as expected (Fig. 4(b)). In absolute values, urea induced a decrease in the ΔV^* of dissociation and a significant increase in the ΔV^* of denaturation.

To obtain information about the secondary structure, we studied the circular dichroism of TMV in the presence of urea, Fig. 4(a) inset. It should be noted that a loss of secondary structure occurs with the increase in urea concentration, which is more accentuated with urea concentrations from 4.0 to 6.0 mol/L. This range is akin to the change in the red shift of fluorescence, Fig. 1(b) inset, confirming the good correlation between fluorescence data and denaturation.

The comparative effect of urea on the dissociation and denaturation of TMV at 0.1, 110 and 220 MPa, Fig. 4(c), shows that, at these pressure values, viral dissociation is observed at lower urea concentrations, compared with viral denaturation, and pressure increases these different susceptibilities (difference of 1.0 mol/L urea at 0.1 MPa, and 2.5 mol/L at 110 MPa). Fig. 4(c) insets show the comparison of light scattering (top) and center of mass (bottom) at the pressure values corresponding to Fig. 4(c).

Gel filtration studies of pressurized TMV (220 MPa for 1.5 h) in the presence of urea were performed to observe the dissociation products. Fig. 5(a) shows the elution profile in the absence of urea as a single peak at V_0. After pressure incubation, gel filtration presents an elution profile compatible with partial dissociation, Fig. 5(a). The presence of 0.5 mmol/L urea did not affect the elution profile of either the control or the pressurized sample (not shown). At higher urea concentrations, increases of viral dissociation were observed, that were more intense at higher urea concentrations and after pressure incubations, Fig. 5(b) and (c).

Electron microscopy provided additional information about the structural organization of TMV under different urea concentrations. Fig. 6(b) shows that the presence of 2.0 mol/L urea induced a smaller number of virus images in the associated form than does the control in the absence of urea, Fig. 6(a). The increase of urea concentration to 3.0 mol/L promotes a much lower number of virus images, with significant fragmentation seen from the smaller sizes of visible particles, Fig. 6(c). The samples incubated at urea concentrations of 4.0 mol/L (Fig. 6(d)) and 7.0 mol/L (not shown) exhibited no viral images in all analyzed fields.

4. Discussion

The molecular mechanism of action of urea destabilization of proteins is not yet totally understood. It is postulated to be due to urea interactions with the polypeptide chain or through solubilization of non-polar groups such as aromatic residues [31]. Several recent reports suggest that the effect of denaturants is not only through the solvent structure, but that a direct interaction with the protein is more important [32–34]. In dissociation processes the same effects should occur, since when an increase of osmotic pressure occurs, the free water concentration decreases, which is in the direction of protein stabilization against dissociation, the opposite to what is generally observed in the presence of urea [35,36]. This direct urea–protein interaction suggests an associated stoichiometry of dissociation and denaturation, analogous to quantitative proposals for analysis of proton dissociation of TMV [23] and of extracellular hemoglobin [22].

Recently Zlotnick [37] discussed the distinction between reversible and irreversible virus capsid assembly, which was observed in different experimental conditions. As mentioned in this report, irreversibility occurs when the backward reaction is too slow to be relevant to observable kinetics, which clearly means a non-equilibrium state,

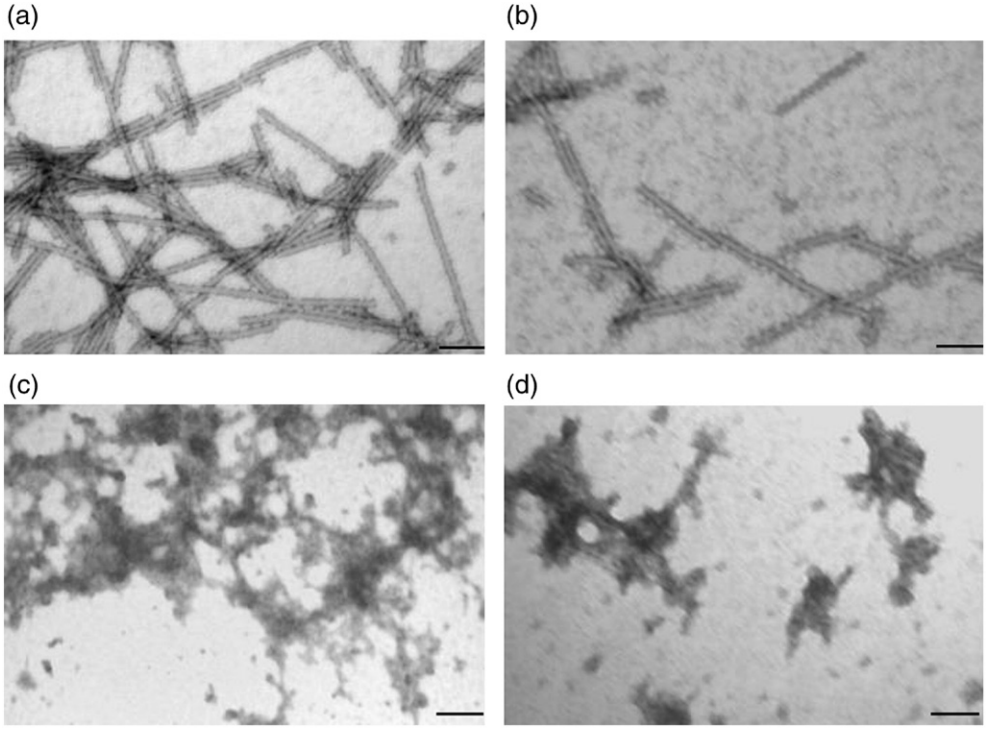

Fig. 6. Transmission electron microscopy of TMV at different urea values. TMV (0.25 mg/mL) was incubated in buffer 100 mmol/L Tris–HCl in pH 7.0 for 1 h at a temperature of 5 °C at (a) an absence of urea, (b) 2.0 mol/L urea, (c) 3.0 mol/L urea and (d) 4.0 mol/L urea. The samples were fixed with 0.5% glutaraldehyde solution. Negative staining was done with 1% uranyl acetate. Bar = 100 nm.

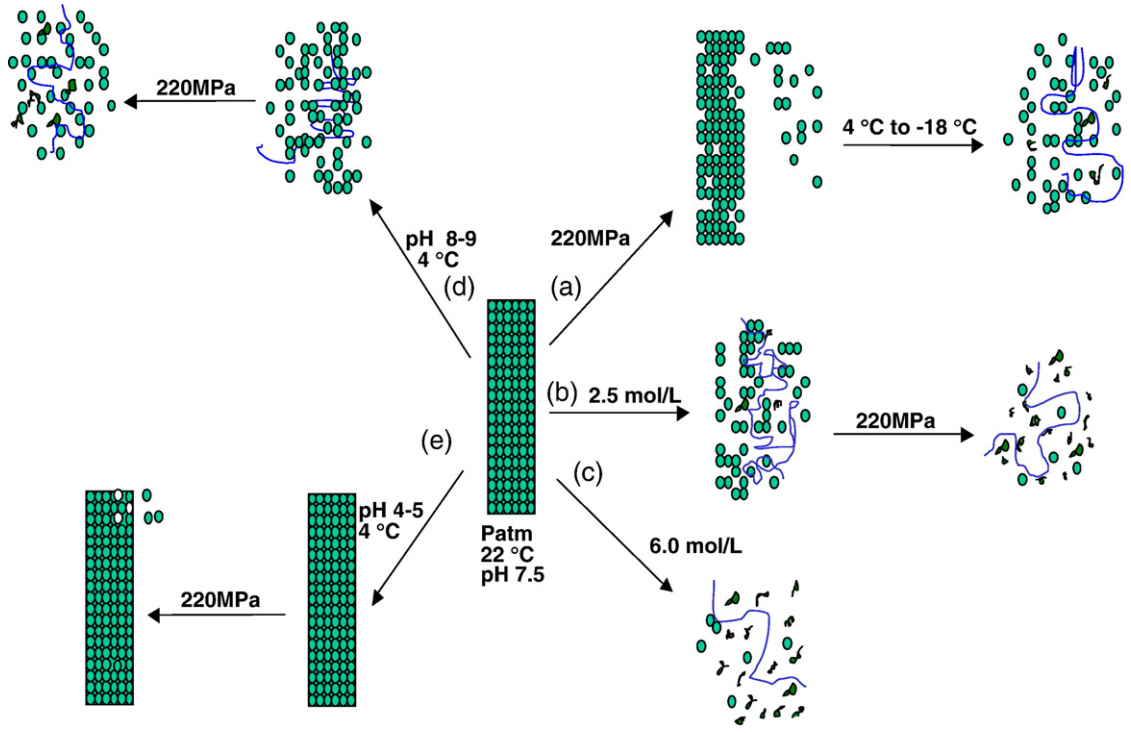

Fig. 7. Dissociation and denaturation processes of TMV under different conditions of pressure, temperature, pH and urea concentrations, based on the present report, Bonafe et al. [9] and Santos et al. [23]. (a) TMV at 220 MPa dissociates slightly, and the temperature decrease (4 °C or lower) induces significant dissociation. (b) Urea at 2.5 mol/L dissociates but does not denaturate TMV, and subsequent pressure incubation induces important denaturation. (c) Urea at 6.0 mol/L induces important dissociation and denaturation. (d) Under alkaline conditions dissociation occurs but no denaturation of viral particles; the former is intensified by pressure incubation. (e) Under acid conditions TMV does not dissociate, even at high hydrostatic pressure.

which is the opposite of the observations using our experimental conditions, where a near equilibrium occurs at each experimental pressurization, Fig. 2(a) and (b). The stabilization of dissociated products suggested that a steady-state approach would be more appropriated, furnishing the apparent thermodynamic parameters.

TMV stability at high pressure has a dependence on physical and chemical conditions such as pressure, temperature, pH and presence of urea, quantified here, and also observed in previous reports [9,23]. Fig. 7 summarizes these findings, showing dissociation and denaturation processes at different conditions. In previous studies, a comparison of disassembly promoted by urea (up to 4.0 mol/L) and alkali incubation of TMV, led to a similar pattern of disassembly under both conditions [38]. Since the urea concentrations were up to 4.0 mol/L in these experiments, the denaturation process should not be significant, so these authors found two different conditions of dissociation leading to similar products, which corresponded to 93%, 68%, 61%, 39%, 31%, 24% and 16% of the total virus length, near 300 nm.

Although the dissociation process could be analyzed based on the different structural species in solution, here we consider a two-state process more adequate to be applied through the light scattering data, as previously performed to study the pH effect of TMV [23]. The degrees of dissociation and denaturation (Fig. 3(a) and (b) inset) obtained from

Table 1
Calculated apparent urea stoichiometry of dissociation and denaturation based on, respectively, light scattering and the center of mass of fluorescence emission spectra data at atmospheric pressure from the literature

Virus	Form	Dissociation stoichiometry	Denaturation stoichiometry	Red shift denaturation	Reference
TMV	Native	1.53; 1.82	11.1; 8.65	1900 cm^{-1}	Present report
TMV	Native	1.48	14.6	2000 cm^{-1}	[9]
R17	Native	5.27 [a]	(9.42)	(1700 cm^{-1})	[6]
R17	Coat protein dimer	0.87 [a]	(4.25)	(1100 cm^{-1})	[6]
Cowpea mosaic virus	Empty capside		6.65	700 cm^{-1}	[7]
Cowpea severe mosaic virus	Native	3.26 [a]	(7.55)	(1000 cm^{-1})	[8]
Poliovirus	Native		5.04	1000 cm^{-1}	[10]
Rhinovirus	Native		11.13	600 cm^{-1}	[10]
Foot and mouth disease virus	Native		5.90	800 cm^{-1}	[10]
P22 bacteriophage	Native shell	0.91	5.60	950 cm^{-1}	[11]
P22 bacteriophage	T294I mutant shell	0.55	3.90	900 cm^{-1}	[11]
Flock house virus	Native	1.30	8.5	1200 cm^{-1}	[12]
Flock house virus	D75N mutant	0.85	7.41	>800 cm^{-1}	[12]
Flock house virus	Native	1.02	6.20	>900 cm^{-1}	[15]
Mayaro virus	Native	0.95	2.63	700 cm^{-1}	[13]
Mayaro virus	Nucleocapside	0.50	1.55	700 cm^{-1}	[13]
Rotavirus	Native		3.91	1000 cm^{-1}	[14]
MS2 bacteriophage	Native		7.22	1800 cm^{-1}	[16]

[a] Dissociation was based on center of mass, in the original reference; the respective stoichiometric value calculated as denaturation is in parenthesis. Underlined values of stoichiometry correspond to calculations based on pressure dissociation curves.

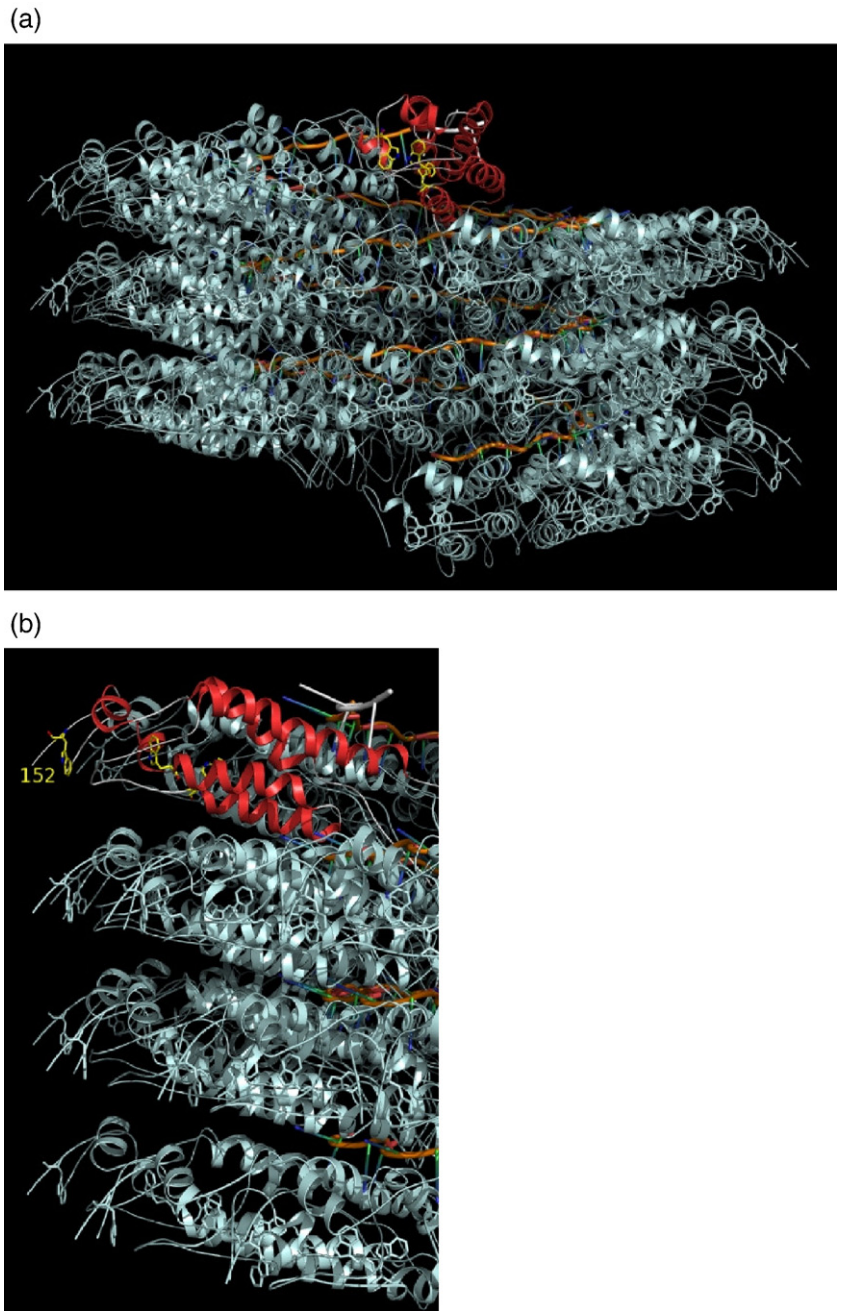

Fig. 8. Cartoon representation of TMV (with smoothed loops). The entire virus is formed by approximately 2130 identical capsid protein subunits arranged in a right-handed helix (pitch equal to 2.3 nm) 300 nm long, with external and internal diameters of 18 and 4 nm, respectively. After reduction by symmetry, a single protein subunit (with three bound nucleotides) summarizes the structural information from the entire virus. (a) A complete helix unit repeat comprising 49 subunits in 3 turns, with one subunit in evidence (alpha helices shown in red); (b) detail emphasizing the location of tryptophan residues (carbon atoms in yellow), in particular, residue 152 at the outer edge of the helix. Drawings were made using PyMOL (DeLano Scientific, San Carlos, CA, http://www.pymol.org) under Linux. (For interpretation of the references to color in this figure legend, the reader is referred to the web version of this article.)

these data furnish quantitative thermodynamic data for both processes at different conditions of urea concentration and pressure. The results from circular dichroism, gel filtration analyses, and electron microscopy, Figs. 4(a) inset, 5 and 6, respectively, were in accordance with the spectroscopic observations. It is important to note that the considered degree of denaturation based on Eq. (3) is very similar to the estimation of denaturation based on circular dichroism, for instance the change of molar ellipticity at 222 nm, Fig. 4(a) inset. The present report confirms previous quantitative studies concerning dissociation and denaturation [9]. A clear distinction between these processes, respectively Fig. 1(a) and (b), could be done based on light scattering and emission fluorescence data. In conditions that induce near total TMV dissociation (220 MPa in the absence or the presence of 0.5 mol/L urea, Fig. 1), the red shift was not detectable, while the red shift in the denaturation process is at 1900 cm^{-1}. Such findings indicate that dissociated forms should preserve the aromatic residues against exposure to solvent. Moreover this red shift value in denaturation is higher than several viruses described in the literature, as listed in Table 1, suggesting a comparatively larger difference of exposure of tryptophans to solvent between the dissociated and denatured form.

In summary, our results indicate that dissociation precedes the denaturation process induced by urea. Fig. 4(c) shows that this tendency is

significantly accentuated by high pressure, so under these conditions the susceptibility of TMV to dissociation increases more than its susceptibility to denaturation. Such behavior should reflect the higher apparent volume change of denaturation comparing to dissociation (in absolute values), with consequent higher sensitivity of TMV to denaturation process at higher pressure.

4.1. Fluorescence spectra in light of the TMV structure

Tryptophan fluorescence is highly sensitive to the surrounding electrostatic environment, a feature that allows for dynamic processes to be studied. Although interpretation of protein emission spectroscopy data is a rather complicated issue, much effort has been applied to relate physical and structural parameters to the tryptophan fluorescence spectra [28,39]. A detailed description of the correlation between the tryptophan environment in the TMV structure with the observed fluorescence spectra is beyond the purpose of this work. Nevertheless, the qualitative approach described below led to remarkable facts relating local structural features of the tryptophans to their contributions to fluorescence during the dissociation and denaturation processes.

An important contribution, Vivian and Callis used a hybrid quantum mechanical–classical molecular dynamics method starting with crystal structures to predict the fluorescence wavelengths of 19 tryptophans in 16 proteins, with calculated λ_{max} within 6 nm of the experimental values [40]. These authors proposed a rough classification of tryptophan environments into five tryptophan classes, with the contribution to the fluorescence red shift increasing with the class number. The classification takes into account the extent of exposure of the faces and edges of the residue to the protein surface: class I — buried, no exposure to water; class II — edge exposed; class III — only one face exposed; class IV — one face and edge exposed; class V — two faces and edge exposed. Aiming to investigate the individual contribution of the tryptophans of the virus coat protein to the fluorescence spectra, this classification was adopted as criteria to distinguish between different environments.

TMV is a rod-shaped virus consisting of approximately 2130 identical capsid protein subunits (17.5 kDa each) assembled in a right-handed helix around a single strand of viral RNA. The capsid protein can also self-assembly in solution and form virus-like rods. The TMV structure, shown in Fig. 8(a), has been determined by X-ray fiber diffraction at 2.9 Angstron resolution (PDB entry 2TMV) [40]. Available structural data also include the crystallographic structure of a four-layer aggregate (2.45 Angstron resolution), a dimer of a bilayered cylindrical disk formed by 34 subunits (PDB entry 1EI7) [41].

The capsid protein has three tryptophans, TRP17, TRP52 and TRP152. These residues were classified as described (Materials and methods), according to the above-mentioned criteria, into classes I to V (Fig. 9).

TRP152, assigned to class IV, is located at the outer edge of the helix, with a side chain almost completely exposed to the solvent in the assembled form of the virus (Fig. 8(b)). At the same time, this residue is near the C-terminal of the protein, a flexible region that exhibits considerable conformational variability, as seen from the structure of the complete TMV, where the last four residues of the carboxy-terminal were not modeled due to disorder, and from the structure of the four-layer aggregate, where the C-terminal is found in different conformations in different subunits (not shown). Conceivably, one should expect that the environment of this tryptophan would not change significantly when comparing the assembled form of the virus and the dissociated capsid protein. For this reason, we expect no significant changes in its contribution to the fluorescence spectra during the dissociation process.

TRP17, buried in the interior of the protein, was classified as a class I tryptophan. No experimental evidence was found that protein unfolding accompanies TMV dissociation. Consequently, we can anticipate that the TRP17 contribution to the spectra would be nearly the same upon dissociation. On the other hand, its contribution is probably much larger for the unfolded than for the native protein. In the case of TRP52, an examination of the structure of the complete virus and the four-layer aggregate shows that, in both cases, this residue has similar environments. Although structural superposition (not shown) indicates a difference in the side chain conformations of this residue in TMV ($\chi1=-102$, $\chi2=-93$) and the four-layer aggregate structure ($\chi1=-47$, $\chi2=101$), the class of the residue is essentially the same (class III). It is important to note that the four-layer aggregate results from the self-assembled capsid protein in solution, which forms virus-like rods. Thus, one can argue that this residue assumes a different conformation (and a higher class) only during the unfolding process.

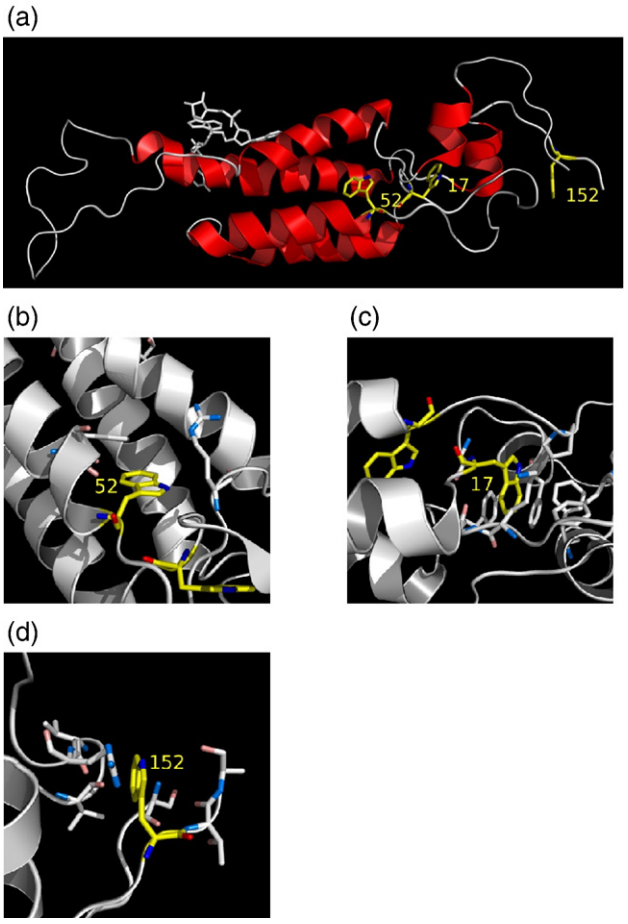

Fig. 9. Tryptophan environments. (a) The capsid protein subunit with an overview of tryptophan local configurations; (b) TRP52 has one face only exposed to the solvent, thus being assigned to class III; (c) TRP17 is completely buried inside the protein and has been classified as pertaining to class I; (d) TRP152, the most exposed to the solvent, has been classified in class IV. Figures were prepared with PyMOL (DeLano Scientific, San Carlos, CA, http://www.pymol.org) under Linux.

In short, our results are in agreement with what would be expected based on structural data. The three tryptophans present in the capsid protein are not expected to exhibit significant structural or class modifications upon dissociation, and accordingly, show no appreciable differences in their fluorescence during dissociation. Moreover, TRP17 and TRP52 are predicted to account for most of the spectral changes observed. TRP152, almost completely exposed to the solvent both in the virus structure and in the capsid protein itself, probably has a minor contribution in both dissociation and denaturation.

4.2. Comparison of urea stoichiometry among viruses and proteins

Previous investigations [9] pointed to similar urea effects on TMV concerning apparent stoichiometry if the approach considered here

(Eqs. (4)–(19)) is applied, with 1.48 mol of urea/mol of TMV subunit for dissociation and 14.6 for denaturation. Here the values found were, respectively, 1.53 and 11.1 mol of urea/mol of subunit. The data from the earlier report should be considered less precise than the present data because the plot of ΔG^* *versus* ln urea concentration was taken from direct atmospheric pressure data, while here we used the ΔG^* values from the pressure curves at different urea concentrations, so the quality should be much better. We show these calculated values in Table 1, also including the apparent urea stoichiometry calculated from atmospheric pressure in the present report, from Fig. 1(a) inset.

Studies of R17 bacteriophage dissociation by urea and pressure compared the viral concentration effect on dissociation at urea concentrations from 2.5 mol/L to 4.5 mol/L, demonstrating that the expected effect of viral dilution in facilitating the dissociation only appears at higher urea concentrations [6]. Concentration independence of viral dissociation in the presence of low urea concentrations (2.5 mol/L) was observed in other macromolecular aggregates such as extracellular hemoglobin [27] and hemocyanin [42]. Erijman and Weber [43] suggested that the lack of protein or virus concentration effects on pressure dissociation is due to the heterogeneity of aggregates, which are present when the number of subunits is higher than two. The urea effect on "recovering" of the viral concentration effect at higher urea concentrations in R17 bacteriophage was explained as a homogenizer effect of urea on the virus [36].

Several viruses under different conditions are described in the literature with respect to the effects of urea on light scattering and the center of mass of fluorescence spectra. For these data, the application of Eqs. (9) and (15), respectively, make it possible to calculate the apparent urea stoichiometry of dissociation or denaturation of such viruses. The results of such calculations are listed in Table 1, which compares these systems. Again, these results are not so refined as the calculation done in the present work because they are based on data at atmospheric pressure only, not on pressure curves. Moreover the data for denaturation process are based on the differences between two very distinct environments for tryptophan residues (red shift of emission fluorescence data for tryptophan exposure to solvent), so other techniques for quantifying denaturation could lead to some variation in the measured stoichiometries. Interestingly, most of the calculated apparent dissociation stoichiometries are in the range of 0.5 to 1.5 mol urea/mol of virus subunit, while for denaturation most of the calculated values are between 4 and 11 mol urea/mol of virus subunit. Among the data of Table 1, only in the investigations involving R17 [6] and cowpea severe mosaic virus, [13] was the criterion for dissociation considered as the red shift of fluorescence spectra, as discussed below.

Mayaro virus and rotavirus presented relatively low apparent urea stoichiometries of denaturation and dissociation. Such results seem to reflect a near linear effect of urea concentration, from 0 to 8 mol/L, in these processes (Fig. 2 from [13], and Fig. 1a from [14]), while in other viruses the urea effect is more abrupt, exhibiting curves with sigmoidal shape, as for TMV (Fig. 1). Rotavirus possesses a more complex organization, in comparison to other icosahedral-symmetry viruses, with a three-shelled structure with different proteins in each, while Mayaro virus is a membrane-enveloped particle. It is possible that, in both viruses, there is a decrease of urea accessibility, spanning the urea effect in the range of 0 to 8 mol/L urea. Comparing an enveloped virus such as Mayaro virus with its nucleocapside form (without its lipid membrane), the apparent stoichiometry was lower in the nucleocapside form. A possible explanation of this finding is that the lipid membrane interaction could induce higher apparent stoichiometry of urea to induce dissociation and denaturation processes compared to other types of viral states.

Although most of the viruses studied used the red shift as a criterion for denaturation, for R17 and cowpea severe mosaic virus, the authors demonstrated that viral dissociation was correlated with red shift changes (6, 8). The calculated apparent stoichiometry of dissociation, respectively 5.27 and 3.26 mol of urea per mol of capsid subunit, are obviously too high, compared to other viruses. If the spectroscopic changes are only due to the denaturation process, the apparent stoichiometry values are similar to other systems (9.42 and 7.55 mol of urea per mol of capside subunit, Table 1, data in parentheses). Denaturation processes were not considered in the original papers, but should have occurred. Thus the center of mass data may reflect changes due to both dissociation and denaturation, which explains the values calculated here. For R17 virus, the comparison of the coat protein dimer with the native form seems to point to a lower apparent urea stoichiometry of dissociation or denaturation of this virus. It is possible that the nucleic acid interaction could induce higher urea stoichiometry of dissociation or denaturation.

An interesting application of our proposal is the investigation of apparent stoichiometry of denaturants on proteins. To illustrate this possibility we used an earlier report involving urea-induced denaturation of human serum albumin [44] calculating the apparent urea stoichiometry. The possibility to extend this approach to other proteins, monomeric or multimeric, should lead to significant results for better understanding the dissociation and denaturation processes. The relevance of this goal can be understood by recalling that the denaturation process is related to several important topics such as protein folding and stability, transport across membranes, proteolysis and protein turnover [45].

In summary, our results point to a similar apparent stoichiometry for urea for dissociation and denaturation, compared to other viruses, which can reflect similar protein–urea interactions. The higher apparent stoichiometry of urea in a denaturation process compared with dissociation is expected since denaturation is much more drastic and should involve many more interactions. On the other hand, it is quite remarkable that only a few molecules of urea per capsid subunit (in some cases less than one) are needed for the dissociation. A reasonable explanation is that both the tubular and spherical particles have their stability controlled at the supramolecular level. Doping the structure with a few molecules of the perturbing agent leads to destabilization. This knowledge can be fundamental for the development of new antiviral approaches.

Acknowledgements

We are grateful to Carol Collins for revising the manuscript, and to Adalberto B.M.S. Bassi for helpful discussions. This work was supported by CNPq (Conselho Nacional de Desenvolvimento Científicoe Tecnológico), FAPESP (Fundação de Amparo à Pesquisa do Estado de São Paulo), CAPES (Coordenação de Aperfeiçoamento de Pessoal de Nível Superior), and FAEPEX–UNICAMP (Fundo de Apoio ao Ensino, Pesquisa e Extensão-Universidade Estadual de Campinas).

References

[1] J.L. Silva, G. Weber, Pressure stability of proteins, Annu. Rev. Phys. Chem. 44 (1993) 89–113.
[2] G. Weber, H.G. Drickamer, The effect of high pressure upon proteins and other biomolecules, Q. Rev. Biophys. 16 (1983) 89–112.
[3] G. Weber, Phenomenological description of the association of protein subunits subjected to conformational drift. Effects of dilution and of hydrostatic pressure, Biochemistry 25 (1986) 3626–3631.
[4] J.L. Silva, A.C. Oliveira, A.M.O. Gomes, L.M.T.R. Lima, R. Mohana-Borges, A.B.F. Pacheco, D. Foguel, Pressure induces folding intermediates that are crucial for protein–DNA recognition and virus assembly, Biochim. Biophys. Acta 1595 (2002) 250–265.
[5] C. Balny, What lies in the future of high-pressure bioscience? Biochim. Biophys. Acta 1764 (2006) 632–639.
[6] A.T. Da Poian, A.C. Oliveira, L.P. Gaspar, J.L. Silva, G. Weber, Reversible pressure dissociation of R17 bacteriophage. The physical individuality of virus particles, J. Mol. Biol. 231 (1993) 999–1008.
[7] A.T. Da Poian, J.E. Johnson, J.L. Silva, Differences in pressure stability of the three components of cowpea mosaic virus: implications for virus assembly and disassembly, Biochemistry 33 (1994) 8339–8346.
[8] L.P. Gaspar, J.E. Johnson, J.L. Silva, A.T. Da Poian, Partially folded states of the capsid protein of cowpea severe mosaic virus in the disassembly pathway, J. Mol. Biol. 273 (1997) 456–466.

[9] C.F.S. Bonafe, C.M.R. Vital, R.C.B. Telles, M.C. Gonçalves, M.S.A. Matsuura, F.B. Pessine, D.R.C. Freitas, J. Vega, Tobacco mosaic virus disassembly by high hydrostatic pressure in combination with urea and low temperature, Biochemistry 37 (1998) 11097–11105.
[10] A.C. Oliveira, D. Ishimaru, R.B. Goncalves, T.J. Smith, P. Mason, D. Sa-Carvalho, J.L. Silva, Low temperature and pressure stability of picornaviruses: implications for virus uncoating, Biophys. J. 76 (1999) 1270–1279.
[11] P. Sousa, R. Tuma, P.E. Prevelige, J.L. Silva, D. Foguel, Cavity defects in the procapsid of bacteriophage P22 and the mechanism of capsid maturation, J. Mol. Biol. 287 (1999) 527–538.
[12] A.C. Oliveira, A.M. Gomes, F.C. Almeida, R. Mohana-Borges, A.P. Valente, V.S. Reddy, J.E. Johnson, J.L. Silva, Virus maturation targets the protein capsid to concerted disassembly and unfolding, J. Biol. Chem. 275 (2000) 16037–16043.
[13] L.P. Gaspar, A.F. Terezan, A.S. Pinheiro, D. Foguel, M.A. Rebello, J.L. Silva, The metastable state of nucleocapsids of enveloped viruses as probed by high hydrostatic pressure, J. Biol. Chem. 276 (2001) 7415–7421.
[14] L. Pontes, Y. Cordeiro, V. Giongo, M. Villas-Boas, A. Barreto, J.R. Araujo, J.L. Silva, Pressure-induced formation of inactive triple-shelled rotavirus particles is associated with changes in the spike protein VP4, J. Mol. Biol. 307 (2001) 1171–1179.
[15] W.D. Schwarcz, S.P.C. Barroso, A.M.O. Gomes, J.E. Johnson, A. Schneemann, A.C. Oliveira, J.L. Silva, Virus stability and protein-nucleic acid interaction as studied by high-pressure effects on nodaviruses, Cell. Mol. Biol. 50 (2004) 419–427.
[16] S.M.B. Lima, A.C.Q. Vaz, T.L.F. Souza, D.S. Peabody, J.L. Silva, A.C. Oliveira, Dissecting the role of protein–protein and protein–nucleic acid interactions in MS2 bacteriophage stability, FEBS J. 273 (2006) 1463–1475.
[17] C.F.S. Bonafe, M. Glaser, E.W. Voss, G. Weber, J.L. Silva, Virus inactivation by anilinonaphthalene sulfonate compounds and comparison with other ligands, Biochem. Biophys. Res. Commun. 275 (2000) 955–961.
[18] D. Ishimaru, D. S-Carvalho, J.L. Silva, Pressure-inactivated FMDV: a potential vaccine, Vaccine 22 (2004) 2334–2339.
[19] P. Goelet, G.P. Lomonossoff, P.J. Butler, M.E. Akam, M.J. Gait, J. Karn, Nucleotide sequence of tobacco mosaic virus RNA, Proc. Natl. Acad. Sci. U. S. A. 79 (1982) 5818–5822.
[20] W.M. Stanley, M.A. Lauffer, Disintegration of tobacco mosaic virus in urea solution, Science 89 (1939) 345–347.
[21] L.E. Blowers, T.M.A. Wilson, The effect of urea on tobacco mosaic virus-polarity of disassembly, J. Gen. Virol. 61 (1982) 137–141.
[22] J.A.C. Bispo, J.L.R. Santos, G.F. Landini, J.M. Goncalves, C.F.S. Bonafe, pH dependence of the dissociation of multimeric hemoglobin probed by high hydrostatic pressure, Biophys. Chemist. 125 (2007) 341–349.
[23] J.L.R. Santos, J.A.C. Bispo, G.F. Landini, C.F.S. Bonafe, Proton dependence of tobacco mosaic virus dissociation by pressure, Biophys. Chemist. 111 (2004) 53–61.
[24] A. Asselin, M. Zaitlin, Characterization of a second protein associated with virions of tobacco mosaic virus, Virology 91 (1978) 173–181.
[25] A.A. Paladini, G. Weber, Absolute measurements of fluorescence polarization at high pressures, Rev. Sci. Instrum. 52 (1981) 419–427.
[26] C. Tanford, Physical Chemistry of Macromolecules, Wiley, 1961.
[27] J.L. Silva, M. Villas-Boas, C.F.S. Bonafe, N.C. Meirelles, Anomalous pressure dissociation of large protein aggregates. Lack of concentration dependence and irreversibility at extreme degrees of dissociation of extracellular hemoglobin, J. Biol. Chem. 264 (1989) 15863–15868.
[28] J.T. Vivian, P.R. Callis, Mechanisms of tryptophan fluorescence shifts in proteins, Biophys. J. 80 (2001) 2093–2109.
[29] M. Winn, E.J. Dodson, A. Ralph, Collaborative computational project, number 4: providing programs for protein crystallography, Method. Enzymol. 277 (1997) 620–633.
[30] B.H. Lavenga, Thermodynamics of Irreversible Processes, The Macmillan Press Ltd., London, 1978.
[31] J.M. Scholtz, D. Barrick, E.J. York, J.M. Stewart, R.L. Baldwin, Urea unfolding of peptide helices as a model for interpreting protein unfolding, Proc. Natl. Acad. Sci. U. S. A. 92 (1995) 185–189.
[32] F. Vanzi, B. Madan, K. Sharp, Effect of the protein denaturants urea and guanidinium on water structure: A structural and thermodynamic study, J. Am. Chem. Soc. 120 (1998) 10748–10753.
[33] A.W. Omta, M.F. Kropman, S. Woutersen, H.J. Bakker, Negligible effect of ions on the hydrogen-bond structure in liquid water, Science 301 (2003) 347–349.
[34] J.D. Batchelor, A. Olteanu, A. Tripathy, G.J. Pielak, Impact of protein denaturants and stabilizers on water structure, J. Am. Chem. Soc. 126 (2004) 1958–1961.
[35] C.R. Robinson, S.G. Sligar, Hydrostatic pressure reverses osmotic pressure effects on the specificity of EcoRI–DNA interactions, Biochemistry 33 (13) (1994) 3787–3793.
[36] G. Weber, A.T.D. Poian, J.L. Silva, Concentration dependence of the subunit association of oligomers and viruses and the modification of the latter by urea binding, Biophys. J. 70 (1996) 167–173.
[37] A. Zlotnick, Distinguishing reversible from irreversible virus capsid assembly, J. Mol. Biol. 366 (1) (2007) 14–18.
[38] R. Hogue, A. Asselin, Study of tobacco mosaic-virus in vitro disassembly by sucrose density gradient centrifugation and agarose-gel electrophoresis, Can. J. Bot. 62 (1984) 457–462.
[39] Y.K. Reshetnyak, E.A. Burstein, Decomposition of protein tryptophan fluorescence spectra into log-normal components. II. The statistical proof of discreteness of tryptophan classes in proteins, Biophys. J. 81 (2001) 1710–1734.
[40] K. Namba, R. Pattanayek, G. Stubbs, Visualization of protein–nucleic acid interactions in a virus. refined structure of intact tobacco mosaic virus at 2.9 a resolution by X-ray fiber diffraction, J. Mol. Biol. 208 (1989) 307–325.
[41] B. Bhyravbhatla, S.J. Watowich, D.L. Caspar, Refined atomic model of the four-layer aggregate of the tobacco mosaic virus coat protein at 2.4—a resolution, Biophys. J. 74 (1998) 604–615.
[42] C.F.S. Bonafe, J.R.V. Araujo, J.L. Silva, Intermediate states of assembly in the dissociation of gastropod hemocyanin by hydrostatic pressure, Biochemistry 33 (1994) 2651–2660.
[43] L. Erijman, G. Weber, Oligomeric protein associations: transition from stochastic to deterministic equilibrium, Biochemistry 30 (1991) 1595–1599.
[44] B. Ahmad, M.K.A. Khan, S.K. Haq, R.H. Khan, Intermediate formation at lower urea concentration in b isomer of human serum albumin: a case study using domain specific ligands, Biochem. Biophys. Res. Commun. 314 (2004) 166–173.
[45] K.A. Dill, D. Shortle, Desnatured states of proteins, Annu. Rev. Biochem. 60 (1991) 795–825.